

Calibration of charge state conversion surfaces for neutral particle detectors

P. Wahlström,^{1,a)} J. A. Scheer,¹ P. Wurz,¹ E. Hertzberg,² and S. A. Fuselier²

¹Physikalisches Institut, University of Bern, Sidlerstrasse 5, 3012 Bern, Switzerland

²Lockheed Martin Advanced Technology Center, 3251 Hanover St., Palo Alto, California 94304, USA

(Received 24 September 2007; accepted 16 May 2008; published online 1 August 2008)

Molecular oxygen and hydrogen ions were scattered off hydrogen terminated diamondlike carbon (DLC) charge state conversion surfaces at incident grazing angles. The energy range of the scattered particles was 390–1000 eV, and the surface roughness of the DLC surface was of the order of 1 Å rms. For all surfaces almost equal angular scattering and negative ion fractions were found within the uncertainties of the measurement. This result supports the fact that charge state conversion with DLC surfaces is a reliable technology for neutral particle sensing instruments. Furthermore, these instruments can work in the laboratory as well as in the harsh environment on board a satellite. The surfaces measured here are used in the IBEX-lo sensor, a neutral particle sensing instrument on the NASA IBEX mission, which is scheduled for launch into orbit around Earth in July 2008. © 2008 American Institute of Physics. [DOI: 10.1063/1.2957064]

I. INTRODUCTION

The interaction of atomic and molecular particles with insulating surfaces has been researched extensively in recent years.^{1–10} Reports of relatively high fractions of negative ions that result from scattering of positive atomic and molecular ions off insulating surfaces have suggested possibilities for several new applications. Currently, we use this process for efficient detection of 10 eV–2 keV neutral particles in interplanetary and interstellar space.^{11–13} The proof of concept for this detection technique has already been demonstrated with the IMAGE mission.¹⁴ The mass spectrograph used there is designed to detect low energy neutral atoms. It uses a conversion surface of volatile adsorbates on a highly polished polycrystalline tungsten substrate to convert a fraction of the incoming neutral atoms into negatively charged ions.^{14,15} For future missions, such as the NASA IBEX mission, diamondlike carbon surfaces will be used as conversion surfaces because of their better long-term stability and higher negative ion yield.^{9,10,16}

Nine flight-spares and nonflight hydrogen terminated diamondlike carbon surfaces have been tested for their negative ionization efficiencies and their angular scattering properties. The dependency of these two properties on the incident angle of the particles was investigated. These surfaces are identical to all 28 trapezoid-shaped (2.5 cm and 2.9×6.2 cm²) neutral to negative conversion surfaces, which will be used for the IBEX mission. Obviously, surfaces with nearly identical scattering properties, i.e., angular scattering and ion conversion efficiency, are required.

Since interstellar gas is expected to consist mainly of H and He with traces of O, N, C, and Ne,¹⁷ we focused our tests on these particles. Measurements of the fraction of negative ions produced upon scattering were performed with O and H. He and Ne cannot produce stable negative ions.

However, He can produce a metastable negative ion.¹⁸ The yield of negative He ions upon surface scattering is of the order of 10^{-5} ,¹⁹ which is several orders of magnitude lower than the sputter yield of negative ions. Thus, negative ion yields measured by scattering He and Ne on charge state conversion surfaces are dominated by several orders of magnitude by the sputtered yield in this experiment. Therefore He and Ne were used to determine the sputtering yields.

In the case of hydrogen and oxygen, molecular ions were used because they can be produced far more efficiently than atomic ions in our test system. The impact of using positively charged molecular ions on the results is discussed in detail below.

II. EXPERIMENT

The Si wafers used as substrates for the tetrahedral amorphous carbon (ta-C) films are 1 mm thick with the $\langle 100 \rangle$ face exposed and boron doped for conductivity in the 1–20 Ω cm range. Cut and polished wafer surfaces were measured to be within 0.13° of the actual $\langle 100 \rangle$ lattice plane. The ta-C thin films were prepared by pulsed laser deposition using an excimer laser (248 nm, Lambda Physik Compex® 150 configured in the power oscillator power amplifier mode) at high fluence (~ 100 J/cm²) to ablate a pyrolytic graphite target in vacuum ($< 1 \times 10^{-6}$ mbar). Under these conditions the ablated carbon flux is highly ionized with a broad energy distribution ranging from 20 to 300 eV. The carbon ions penetrate and implant in the near surface region (called subplantation²⁰) causing densification and build up of stress, ultimately leading to high fourfold (i.e., sp^3 -bonded) carbon content measured at $> 80\%$ (Ref. 21) of the amorphous films. The subplantation also suppresses surface diffusion, which is thought to be one reason why these films are so smooth. Electrical conductivity^{22,23} depends sensitively on the amount of threefold (i.e., sp^2 -bonded) coordinated carbon present, and the degree of clustering and/or chain formation. The electron conduction is accomplished by hopping from

^{a)}Author to whom correspondence should be addressed. FAX: +41-31-631-4405. Electronic mail: peter.wahlstroem@space.unibe.ch.

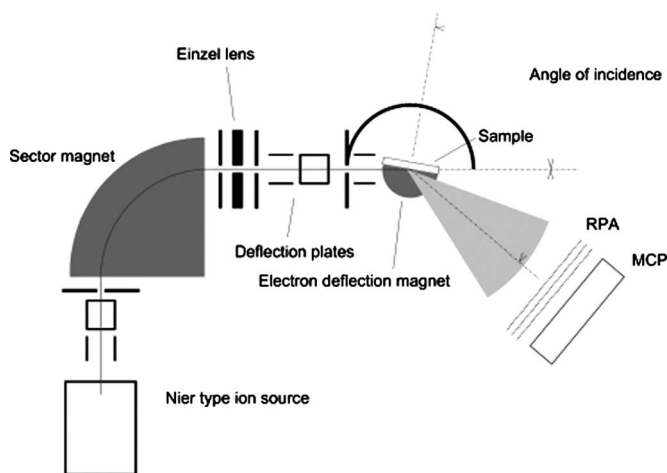


FIG. 1. Schematic diagram of the ILENA experiment. A positively charged ion beam is produced in a Nier-type ion source with energies of ~ 100 up to 1200 eV. The beam then passes through an electromagnet that allows the selection of the desired species. The sample surface is mounted on a revolvable sample holder which allows angles of incidence of 0° – 90° . The MCP can be turned freely around the same axis.

threefold clusters mediated by the cluster size and spacing. Typically, resistivities of $10^6 \Omega \text{ cm}$ are found for high fourfold content films, but resistivities have been measured down to $10 \Omega \text{ cm}$ in annealed films with slightly lower fourfold content.

The surfaces have been hydrogen terminated because at the surface each carbon atom has one free bonding site that is very reactive. The hydrogen termination process saturates all free bonding sites and thus creates a chemically very stable surface. Furthermore, the negative ion fraction is known to increase slightly after the hydrogen termination.¹⁶ Due to the rather high base pressure of 5×10^{-8} mbar in the vacuum chamber used in this experiment, differences between hydrogen terminated and nonhydrogen terminated surfaces are difficult to identify because a layer of adsorbed hydrogen on the surfaces is almost inevitable.

Surface smoothness is critical for minimizing scattering losses in the downstream particle collection and analysis system of any test apparatus or instrument. The exceptional smoothness of these ta-C samples, approaching perfect smoothness ($<1 \text{ \AA rms}$) when processed optimally, was an important criterion in selecting this material.

The measurements presented here were made with the imager for low energetic neutral atom (ILENA) apparatus at the University of Bern, Switzerland. The setup is described briefly. More details on the experimental setup can be found elsewhere.^{11,24} ILENA consists of an ion source, a magnetic beam filter, an ion guiding system, a sample stage with housing, and a detection unit. All these units are contained in a single vacuum chamber pumped by an ion getter pump. A schematic diagram of the setup is shown in Fig. 1.

The reflected beam is recorded using a two-dimensional position-sensitive microchannel plate (MCP) detector with a viewing angle of $\pm 12.5^\circ$ in both azimuthal and polar directions. A retarding potential analyzer (RPA) consisting of three grids is mounted in front of the MCP detector. The detector unit, including the RPA, is shielded electrostatically

and can be rotated independently of the converter surface around the same axis as the converter surface. The outer grids of the RPA are grounded to shield the inner grid, which can be biased to suppress positive ions. An additional grid in front of the MCP detector at negative potential with respect to the MCP detector serves to reject secondary electrons originating from the preceding grids and the converter surface. The MCP detector may be floated to a high negative voltage with respect to the converter surface to vary the transmission threshold for negative particles. After baking out the vacuum chamber at 80°C for one day, a residual gas pressure of 5×10^{-8} mbar is achieved. During operation the pressure may rise into the low 10^{-7} mbar range as a result of test gas leaking into the ion source chamber. This pressure mirrors the conditions within a typical particle sensing satellite instrument shortly after launch. From the ROSETTA mission of the European Space Agency, it is known that several weeks after launch, the pressure in the vicinity of the spacecraft drops to the low 10^{-9} mbar range, and into the 10^{-11} mbar range after one year.²⁵ The pressure inside space instruments with small openings to vent to the outside, such as most particle instruments, is expected to be at least an order of magnitude higher than the pressure outside the spacecraft. Because of internal outgassing, pressures in the 10^{-8} mbar range are expected to persist in space particle instruments more or less indefinitely.

The fraction of negative ions is determined by taking measurements with and without an applied floating voltage on the MCP. In the first case, only neutral particles are recorded, in the latter, neutral particles and negative ions. From the difference the fraction of negative ions is evaluated.

Each data point results from a series of successive measurements that allow the detection of possible ion beam instabilities and surface charging during each measurement series. With the MCP detector, we cannot distinguish between negatively ionized primary particles and sputtered negative ions. Therefore, measurements with incident positive noble gas ions of comparable mass were performed, e.g., Ne^+ for O^+ , and the negative ion fractions recorded there were taken as an indication of the sputtering background of the previous measurements.

Although we eventually want to use neutral atoms to study surface ionization, for the hydrogen and oxygen measurements we used positive molecular ions because they can be produced far more efficiently and with much better energy, intensity, and angle control in our system than neutrals. However, the charge and mass of molecules must be justified.

From previous experiments with several other insulating surfaces [polycrystalline diamond,¹¹ single-crystal diamond,^{26,27} and MgO (Ref. 12)], it has been established that incident hydrogen and oxygen ions are effectively neutralized upon scattering. These previous measurements were done with both incident positive ions and incident neutral particles and they revealed the same negative ion fractions in both cases. As a result, we can assume complete memory loss of the incident charge state after scattering.

The use of molecules instead of atoms is justified as follows. A molecule has a lot more electronic states than an

atom, so we cannot expect the charge exchange process while scattering to be identical. In separate studies,^{10,11} it has been demonstrated that more than 80% of molecules with energies 300–1000 eV dissociate shortly before reaching the surface when scattered off a polycrystalline diamond surface. As a consequence, the final charge state fraction is determined mainly by charge exchange processes between the surface and dissociated atoms. Therefore, we conclude that the use of molecules causes a negligible change to the charge state fractions measured in this study. In addition, various measurements with different surfaces have shown that the results gained here with energies of 390–1000 eV are comparable to the results which are achieved with incident hydrogen and oxygen atoms with energies of 195–500 eV.

The detection efficiency of the MCP is taken from a previous study^{28,29} in which an identical detector was used.

III. RESULTS AND DISCUSSION

The two key performance requirements for the application of conversion surfaces in neutral particle sensing instruments are high ionization yield and low angular scattering, the latter to minimize scattered particle loss in the detection systems of the sensor. In general, neutral particle sensing instruments use more than one conversion surface. As a consequence, it is essential for accurate measurements that all surfaces used in the instrument show equal performance in the two key requirements.

In the IBEX-lo sensor, 28 circularly arranged charge state conversion surfaces are used. More details on the IBEX-lo sensor can be found elsewhere.^{30,31}

A. Angular scattering

The angular scattering properties of the surfaces are verified by measuring the angular full width at half maximum (FWHM) of the scattered particle beam. The component of angular deviation from specular reflection that resides in a plane containing the incoming trajectory and is normal to the surface is defined as polar scattering. The scattering component normal to the polar angle plane is defined as the azimuthal scattering with zero indicating a true specular reflection.

The measured angular scattering dependence on surface roughness for different IBEX conversion surfaces is shown in Fig. 2. The rms roughness of the surfaces has been measured with an atomic force microscope (AFM).³²

The scattering angles in azimuthal direction are generally larger than the scattering angles in polar direction and the FWHM increases significantly with increasing energy. However, a dependency on the surface roughness cannot be seen here. The variations in the angular FWHM measured for surfaces with different (rms) surface roughness are almost within the measurement uncertainty of $\pm 1^\circ$ for ILENA, as can be seen in Fig. 2, and there is no noticeable trend. With the ILENA apparatus it is not possible to find a dependency of the scattering properties on the very small variations in the surface roughness measured with the AFM.

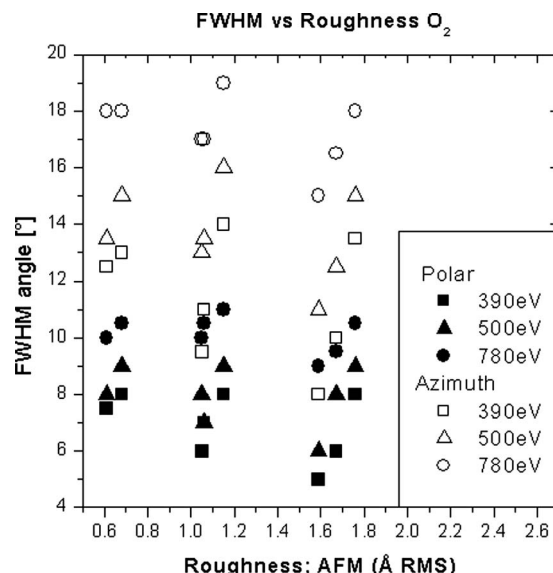


FIG. 2. Surface roughness (rms) measured with an AFM for the IBEX-lo conversion surfaces vs angular FWHM in polar and azimuthal directions of a scattered O_2 beam for energies of incident molecular ions of 390, 500, and 780 eV. The FWHM decreases with decreasing energy of the incident particle and is narrower in polar direction than in azimuthal direction. No dependence on the surface roughness can be seen.

B. Angular dependency

For most of the measurements presented in this paper, the angle of incidence of the ion beam is 8° with respect to the surface plane. This was chosen because all previous measurements during the selection process of the charge state conversion surfaces were done with this setting, even before the angle of incidence in the IBEX-lo sensor was known. To obtain comparable results, the angle of incidence was kept at the same value. In the IBEX-lo instrument the angle of incidence is 15° with respect to the surface plane and the field of view is $\pm 7^\circ$. Therefore, the dependence of the angular scattering and the fraction of negative ions on the angle of incidence were tested.

The influence of the incidence angle on the scattered beam can be seen in the pictures taken with the imaging detector, as shown in Fig. 3. The three pictures show a 500 eV O_2 beam scattered off an IBEX-lo charge state conversion surface with different angles of incidence. The beam profile broadens with increasing angle of incidence. The base height of the profile also increases with increasing angle of incidence. At an angle of incidence of 2° relative to the surface plane, the plateau of almost isotropic scattering can be observed at about 5%. At 8° the flanks of the scattered peak nearly reach the limit of the field of view of the detector; thus the plateau can only be estimated to be between 10% and 15%. The last profile shown in Fig. 3 shows an even broader distribution where the plateau is completely masked by the flanks of the scattered peak. It is therefore only possible to give an upper limit of the base height at 12° of about 30%.

In Figs. 4 and 5 the FWHM dependency on the angle of incidence is shown. The FWHM increases considerably with increasing angle of incidence relative to the surface plane and also with increasing energy of the scattered particles.

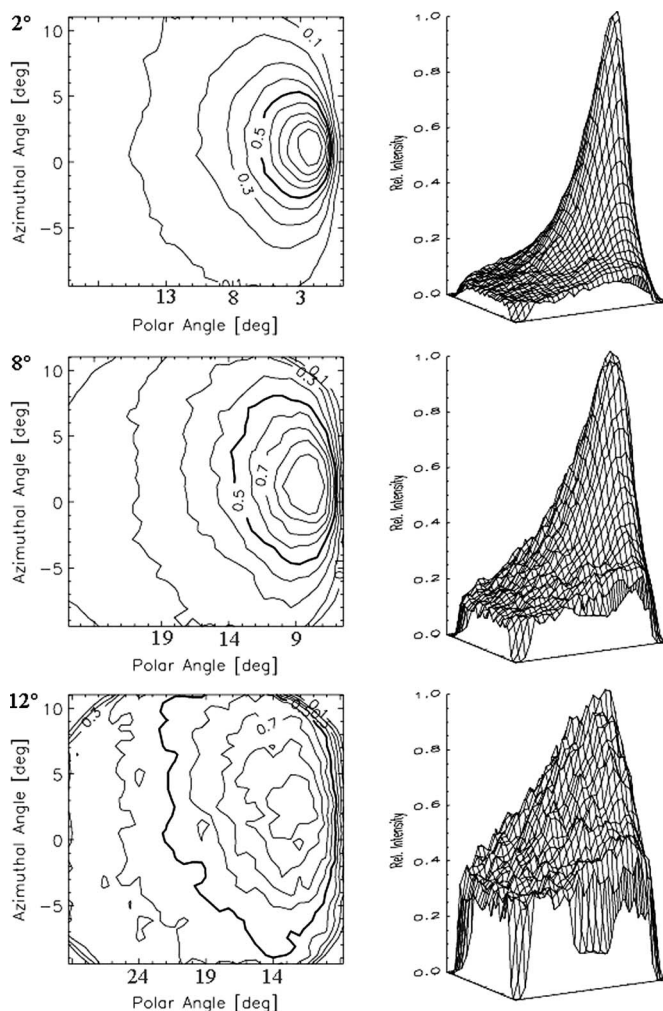


FIG. 3. Scattering images and profiles of a 500 eV O_2 beam scattered under various angles of incidence (2° , 8° , and 12° with respect to the surface plane).

C. Ionization yield

The negative ion yields measured for scattering of molecular hydrogen and oxygen ions off the IBEX-lo charge

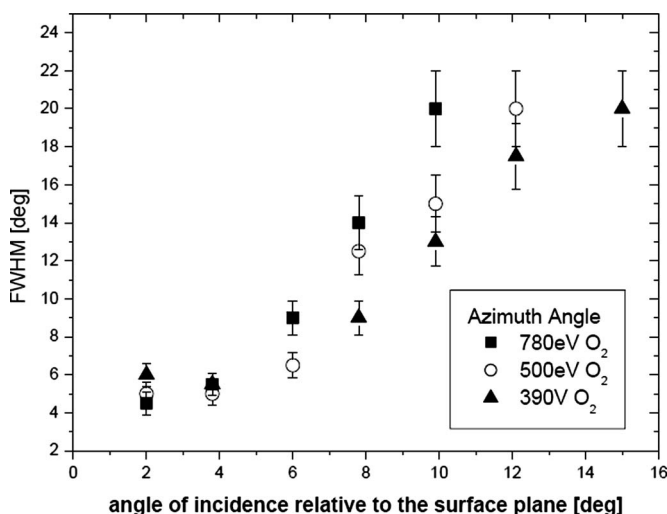


FIG. 4. FWHM in azimuthal direction of the distribution of particles scattered from an IBEX charge state conversion surface for various angles of incidence.

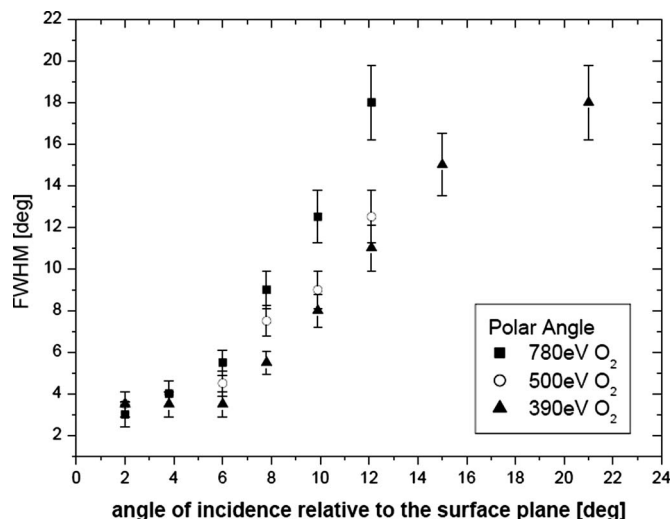


FIG. 5. FWHM in polar direction of the distribution of particles scattered from an IBEX charge state conversion surface for various angles of incidence.

state conversion surfaces are shown in Fig. 6. We found increasing negative charge state fractions with increasing energy of the incident ions. Similar findings have been reported for other insulating surfaces like MgO ,¹² LiF ,⁸ and $BaZrO_3$.³³

For hydrogen we recorded negative ion yields of about 2%–4% and for oxygen about 11%–19%. Projectiles incident on different IBEX charge state conversion surfaces, with a given energy, give rise to equally high negative ion yields for all surfaces within the experimental uncertainties.

D. Angular dependency

The dependency of the negative ion yield on the angle of incidence has also been investigated. The fraction of negative ions versus the velocity component normal to the surface is shown in Fig. 7. As a first approximation, the negative ion yield depends only on the velocity normal to the surface and thus no difference between the particles with different primary energies should be seen. The time during which elec-

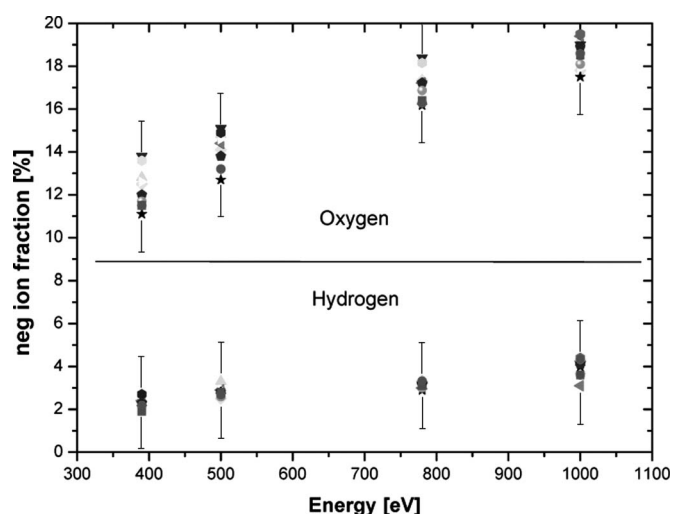


FIG. 6. Ionization efficiencies of all measured IBEX charge state conversion surfaces indicated by the different symbols. The error bars for all measurements include statistical and experimental uncertainties.

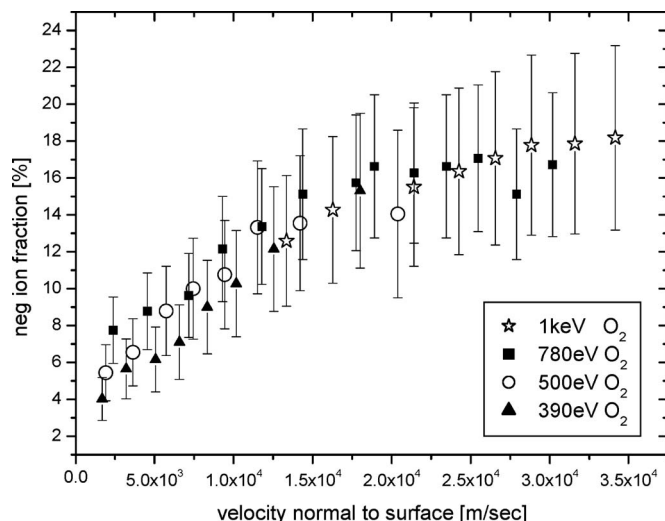


FIG. 7. Fraction of negative ions produced by an O_2 beam scattered from IB0064 is shown as dependent on the velocity normal to the surface.

tronic processes can occur depends strongly on the velocity normal to the surface. This is reflected in the measurements. The ionization yield also depends on the velocity parallel to the surface at high parallel velocities, which was explained via a kinetic resonance (Winter⁷). This effect is less important for our experimental setup. The data show a clear trend of increasing fractions of negative ions up to a level of roughly 23%, which is reached at a normal velocity of 20 km/s. When increasing the normal velocity further, the yield remains stable within the measurement uncertainty. No trend for further increasing or decreasing negative ion yield has been found here. However the error bars allow different interpretations of the measurements.

E. Summary

As expected the distribution of scattered particles broadens with increasing angles of incidence relative to the surface plane. This can be understood due to the increase in kinetic energy perpendicular to the surface with increasing angle of incidence. Particles with higher kinetic energies normal to the surface penetrate into deeper levels of the surface potential where the corrugation of the potential is larger, resulting in larger angular scattering distributions (Figs. 3–5).

The same effect can be seen for particles with different kinetic energies for a constant angle of incidence. The distribution broadens with increasing kinetic energies as this also includes an increase in the kinetic energy normal to the surface.

The fraction of negative ions produced by scattering neutrals or positive ions from a charge state conversion surface depends on the kinetic energy of the particle and the angle of incidence. The negative ion yield increases with increasing kinetic energy normal to the surface, thus with increasing angle of incidence with respect to the surface plane and with increasing overall kinetic energy of the particle, as seen in Figs. 6 and 7. It has been suggested^{8,12,33} that higher energies cause smaller distances of closest approach

TABLE I. Arithmetic mean and standard deviation for different energies for an angle of incidence of 8° . The negative ion fraction is given for hydrogen and oxygen molecules, whereas the FWHM is only shown for oxygen molecules in polar and azimuthal directions. All values are given with statistical error.

Energy (eV)	Neg. ion fraction (%)		FWHM O_2 (deg)	
	H_2	O_2	Polar	Azimuth
1000	3.9 ± 0.4	18.6 ± 0.7	11.1 ± 0.7	18.8 ± 1.3
780	3.1 ± 0.2	17.1 ± 0.7	9.7 ± 1.1	16.9 ± 1.5
500	2.8 ± 0.2	14.1 ± 0.8	7.7 ± 1.2	13.1 ± 1.9
390	2.3 ± 0.2	12.3 ± 0.9	6.7 ± 1.3	11.2 ± 2.2

between scattered ions and surface atoms, which results in higher probabilities for charge exchange processes and thus higher fractions of negative ions.

In Table I the arithmetic mean and the standard deviation is shown for the angular scattering and the fraction of negative ions produced. The angle of incidence was 8° with respect to the surface plane. The similarity of the results for all surface samples and the low angular scattering demonstrates that the key requirement of a similar and smooth (~ 1 Å rms as measured in Ref. 32) surface for all conversion facets with good angular scattering properties is satisfied.

As seen in Fig. 6 and Table I the negative ion yields are equal within the uncertainties of the experiment and the values are within the limits posed by the IBEX team for the IBEX-lo sensor. Thus these charge state conversion surfaces satisfy the second key requirement, which also proves the usability of this technology for further space applications.

IV. CONCLUSIONS

We have tested nine charge state conversion surfaces of nonflight and flight-spare quality of the IBEX-lo sensor for their negative ion yield and their angular scattering distributions. The influence of the angle of incidence on these two parameters was investigated. All surfaces measured met the requirements concerning surface roughness (~ 1 Å rms), FWHM, and negative ion yield defined in the instrument specifications. The surfaces are indistinguishable as seen from the ILENA point of view.

As expected, both FWHM and negative ion yield increase with increasing projectile energy. The angular dependency shows a clear trend of decreasing FWHM and thus better transmission through the instrument with decreasing angle of incidence with respect to the surface plane. On the other hand, the negative ion yield decreases with decreasing angle of incidence. Furthermore the charge state conversion surfaces would have to be longer for smaller angles of incidence, which increase the size and the weight of the detector. Therefore, the incident angle for a flight instrument must be a compromise between high transmission and high negative ion yield and has to be within the limits for weight and size of the detector. For the IBEX-lo sensor an angle of incidence of 15° relative to the surface plane was chosen as the best compromise.

The negative ion yield increases with increasing velocity normal to the surface up to about 2.5×10^4 m/s. At higher

energies the negative ion yield remains relatively constant over the range of the energies measured here.

ACKNOWLEDGMENTS

This work is supported by the Swiss National Science Foundation.

- ¹C. Auth, A. G. Borisov, and H. Winter, *Phys. Rev. Lett.* **75**, 2292 (1995).
- ²P. Stracke, F. Wieggershaus, S. Krischok, H. Müller, and V. Kempter, *Nucl. Instrum. Methods Phys. Res. B* **125**, 63 (1997).
- ³S. A. Deutscher, A. G. Borisov, and V. Sidis, *Phys. Rev. A* **59**, 4446 (1999).
- ⁴P. Roncin, J. Villette, J. P. Atanas, and H. Khemliche, *Phys. Rev. Lett.* **83**, 864 (1999).
- ⁵A. G. Borisov and V. A. Esaulov, *J. Phys.: Condens. Matter* **12**, R177 (2000).
- ⁶R. Souda, *Int. J. Mod. Phys. B* **14**, 1139 (2000).
- ⁷H. Winter, *Phys. Rep.* **367**, 387 (2002).
- ⁸J. A. Scheer, P. Wurz, and W. Heiland, *Nucl. Instrum. Methods Phys. Res. B* **212**, 291 (2003).
- ⁹J. A. Scheer, M. Wieser, P. Wurz, P. Bochsler, E. Hertzberg, S. A. Fuselier, F. A. Koeck, R. J. Nemanich, and M. Schleberger, *Nucl. Instrum. Methods Phys. Res. B* **230**, 330 (2005).
- ¹⁰J. A. Scheer, M. Wieser, P. Wurz, P. Bochsler, E. Hertzberg, S. A. Fuselier, F. A. Koeck, R. J. Nemanich, and M. Schleberger, *Adv. Space Res.* **38**, 664 (2006).
- ¹¹P. Wurz, R. Schletti, and M. R. Aellig, *Surf. Sci.* **373**, 56 (1997).
- ¹²M. Wieser, P. Wurz, K. Brünig, and W. Heiland, *Nucl. Instrum. Methods Phys. Res. B* **192**, 370 (2002).
- ¹³P. Wurz, *The Outer Heliosphere: Beyond the Planets* (Copernicus Gesellschaft e. V., Katlenburg-Lindau, 2000), p. 251.
- ¹⁴T. E. Moore, D. J. Chornay, M. R. Collier, F. A. Herrero, J. Johnson, M. A. Johnson, J. W. Keller, J. F. Laudadio, J. F. Lobell, K. W. Ogilvie, P. Rozmarynowski, S. A. Fuselier, A. G. Ghielmetti, E. Hertzberg, D. C. Hamilton, R. Lundgren, P. Wilson, P. Walpole, T. M. Stephen, B. L. Peko, B. van Zyl, P. Wurz, J. M. Quinn, and G. R. Wilson, *Space Sci. Rev.* **91**, 155 (2000).
- ¹⁵P. Wurz, M. R. Aellig, P. Bochsler, A. G. Ghielmetti, E. G. Shelley, S. Fuselier, F. Herrero, M. F. Smith, and T. Stephen, *Opt. Eng.* **34**, 2365 (1995).
- ¹⁶J. A. Scheer, *Surface Ionization at Insulating Surfaces. A Novel Concept to Detect Neutral Particles in Space* (University of Bern, Switzerland, 2005).
- ¹⁷J. Geiss and M. Witte, *Space Sci. Rev.* **78**, 229 (1996).
- ¹⁸B. Brehm, M. A. Gusinov, and J. L. Hall, *Phys. Rev. Lett.* **19**, 737 (1967).
- ¹⁹P. Wurz, L. Saul, J. Scheer, E. Möbius, H. Kucharek, and S. Fuselier, *J. Appl. Phys.* **103**, 054904 (2008).
- ²⁰Y. Lifshitz, S. R. Kasi, and J. W. Rabalais, *Phys. Rev. Lett.* **62**, 1290 (1989).
- ²¹T. M. Alam, T. A. Friedmann, P. A. Schultz, and D. Sebastiani, *Phys. Rev. B* **67**, 245309 (2003).
- ²²J. P. Sullivan and T. A. Friedmann, Proceedings of the 1st International Specialist Meeting on Amorphous Carbon (World Scientific, Singapore, 1998).
- ²³J. P. Sullivan, T. A. Friedmann, R. G. Dunn, E. B. Stechel, P. A. Schultz, and N. Missert, *The Electron Transport Mechanism in Amorphous Tetrahedrally-Coordinated Carbon Films*, MRS Symposia Proceedings No. 498 (Materials Research Society, Pittsburgh, 1998).
- ²⁴S. Jans, P. Wurz, R. Schletti, T. Fröhlich, E. Hertzberg, and S. Fuselier, *J. Appl. Phys.* **87**, 2587 (2000).
- ²⁵S. Graf, K. Altwegg, H. Balsiger, P. Bochsler, B. Fiethe, and E. Montagnon, *J. Spacecr. Rockets* **45**, 57 (2008).
- ²⁶J. A. Scheer, K. Brünig, T. Fröhlich, P. Wurz, and W. Heiland, *Nucl. Instrum. Methods Phys. Res. B* **157**, 208 (1999).
- ²⁷P. Wurz, T. Fröhlich, K. Brünig, J. A. Scheer, W. Heiland, E. Hertzberg, and S. Fuselier, Prague Proceeding Week of Postdoctoral Students, 1998, edited by J. Safrankov and A. Kanka (unpublished), p. 257.
- ²⁸B. L. Peko and T. M. Stephen, *Nucl. Instrum. Methods Phys. Res. B* **171**, 597 (2000).
- ²⁹T. M. Stephen and B. L. Peko, *Rev. Sci. Instrum.* **71**, 1355 (2000).
- ³⁰M. Wieser, P. Wurz, E. Moebius, S. A. Fuselier, E. Hertzberg, and D. J. McComas, *Rev. Sci. Instrum.* **78**, 124502 (2007).
- ³¹N. Lorente, J. Merino, F. Flores, and M. Yu. Gusev, *Nucl. Instrum. Methods Phys. Res. B* **125**, 277 (1997).
- ³²Evans Analytical Group (EAG). Sunnyvale, California, USA.
- ³³S. Jans, P. Wurz, R. Schletti, K. Brünig, K. Sekar, W. Heiland, J. Quinn, and R. E. Leuchter, *Nucl. Instrum. Methods Phys. Res. B* **173**, 503 (2001).